

## Methanol production from CO<sub>2</sub> using solar-thermal energy: process development and techno-economic analysis†

Jiyong Kim,<sup>a</sup> Carlos A. Henaó,<sup>a</sup> Terry A. Johnson,<sup>b</sup> Daniel E. Dedrick,<sup>b</sup> James E. Miller,<sup>c</sup> Ellen B. Stechel<sup>d</sup> and Christos T. Maravelias<sup>\*a</sup>

Received 18th March 2011, Accepted 4th July 2011

DOI: 10.1039/c1ee01311d

We describe a novel solar-based process for the production of methanol from carbon dioxide and water. The system utilizes concentrated solar energy in a thermochemical reactor to reenergize CO<sub>2</sub> into CO and then water gas shift (WGS) to produce syngas (a mixture of CO and H<sub>2</sub>) to feed a methanol synthesis reactor. Aside from the thermochemical reactor, which is currently under development, the full system is based on well-established industrial processes and component designs. This work presents an initial assessment of energy efficiency and economic feasibility of this baseline configuration for an industrial-scale methanol plant. Using detailed sensitivity calculations, we determined that a break-even price of the methanol produced using this approach would be 1.22 USD/kg; which while higher than current market prices is comparable to other renewable-resource-based alternatives. We also determined that if solar power is the sole primary energy source, then an overall process energy efficiency (solar-to-fuel) of 7.1% could be achieved, assuming the solar collector, solar thermochemical reactor sub-system operates at 20% sunlight to chemical energy efficiency. This 7.1% system efficiency is significantly higher than can currently be achieved with photosynthesis-based processes, and illustrates the potential for solar thermochemical based strategies to overcome the resource limitations that arise for low-efficiency approaches. Importantly, the analysis here identifies the primary economic drivers as the high capital investment associated with the solar concentrator/reactor sub-system, and the high utility consumption for CO/CO<sub>2</sub> separation. The solar concentrator/reactor sub-system accounts for more than 90% of the capital expenditure. A life cycle assessment verifies the opportunity for significant improvements over the conventional process for manufacturing methanol from natural gas in global warming potential, acidification potential and non-renewable primary energy requirement provided balance of plant utilities for the solar thermal process are also from renewable (solar) resources. The analysis indicates that a solar-thermochemical pathway to fuels has significant potential, and points towards future research opportunities to increase efficiency, reduce balance of plant utilities, and reduce cost from this baseline. Particularly, it is evident that there is much room for improvement in the development of a less expensive solar concentrator/reactor sub-system; an opportunity that will benefit from the increasing deployment of concentrated solar power (electricity). In addition, significant advances are achievable through improved separations, combined CO<sub>2</sub> and H<sub>2</sub>O splitting, different end products, and greater process integration and distribution. The baseline investigation here establishes a methodology for identifying opportunities, comparison, and assessment of impact on the efficiency, lifecycle impact, and economics for advanced system designs.

<sup>a</sup>Department of Chemical and Biological Engineering, University of Wisconsin, Madison, WI, 53706. E-mail: maravelias@wisc.edu; Fax: +1 608 262 5494; Tel: +1 608 265 9026

<sup>b</sup>Transportation Energy Center, Sandia National Labs, Livermore, CA, 94551

<sup>c</sup>Material Science and Engineering Center, Sandia National Labs, Albuquerque, NM, 87123

<sup>d</sup>Energy Technologies and Systems Solutions Center, Sandia National Labs, Albuquerque, NM, 87123

† Electronic supplementary information (ESI) available. See DOI: 10.1039/c1ee01311d

### 1. Introduction

It is widely recognized that alternatives to petroleum-based fuels are required to ensure the long-term economic and social stability as well as the security and environmental sustainability of the world at large. In the United States, the transportation sector must be given special attention as it accounts for 72% of the 18.8 million barrels of petroleum products consumed each day.<sup>1</sup> While alternative transportation fuels and power generation are being pursued, *e.g.* hydrogen and all electric, the use of

liquid hydrocarbons is likely to persist throughout this century and beyond. Thus, the production of synthetic liquid fuels from carbon-neutral renewable resources can and should be an important part of a diverse energy solution for the future that is both secure and sustainable. In addition, there is growing recognition that sequestering CO<sub>2</sub> is neither the best nor only method to reduce its effects on climate. Rather than treat it as a waste product, CO<sub>2</sub> can also be viewed and utilized as a valuable feedstock or commodity. For example, CO<sub>2</sub> can serve as a feedstock for manufacturing chemicals, or as a solvent or reaction media.<sup>2-7</sup> However, only the production of hydrocarbon fuels, the original source of much of the CO<sub>2</sub>, could utilize the waste product at a scale comparable to current emissions.<sup>8</sup> Of course, in order for there to be a net reduction in CO<sub>2</sub>, it is mandatory that the conversion to hydrocarbon fuels utilizes a sustainable energy source; *e.g.* solar energy. As a feedstock, CO<sub>2</sub> becomes a recyclable carrier for carbon, which when energized can become a secure and renewable solar energy carrier. There are numerous routes and processes in various stages of development to affect the conversion of sunlight, CO<sub>2</sub> and H<sub>2</sub>O into hydrocarbons. Aside from biological and biochemical pathways, the possibilities can very generally be classified as electrochemical, thermochemical, and photochemical. The focus of this paper is the development of a system integrating solar thermochemical conversion to syngas with downstream processing to liquid hydrocarbon fuels.

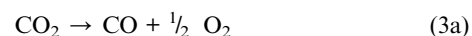
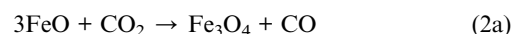
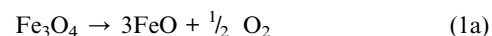
The process described and examined herein is a baseline configuration of an approach now referred to as “Sunshine to Petrol” or “S2P”. At the heart of S2P is a solar thermochemical metal oxide cycle, which for the purposes here is assumed to be implemented as a unique first generation chemical heat engine called the Counter-Rotating-Ring Receiver/Reactor/Recuperator, or CR5. The CR5 combines reduction and oxidation reactions of metal oxides with heat recuperation in a single device based on counter-rotating rings that is thermally driven by solar energy concentrated by a parabolic dish. The initial development of the CR5 was geared solely towards splitting water to produce H<sub>2</sub>.<sup>9,10</sup> In the spring of 2006, the CR5 development effort expanded to include splitting CO<sub>2</sub> to produce CO, and from CO, synthesis gas from water gas shift (WGS) reaction, as a pathway to synthetic hydrocarbon fuels.<sup>11-14</sup> A key insight of this expanded effort is that the CO<sub>2</sub> splitting reaction is entirely analogous to the water splitting reaction. However there are several important distinctions. First, while CO<sub>2</sub> is more stable than H<sub>2</sub>O at low temperatures, it is less stable at temperatures greater than about 800 °C. Thus CO<sub>2</sub> splitting might be accomplished with higher per-pass conversions than H<sub>2</sub>O splitting at higher temperatures where reaction rates are more favorable. Second, because of this cross-over in stability, thermochemical CO production is a potentially convenient and thermodynamically favorable path to H<sub>2</sub> production and eventually hydrocarbon fuels through the low temperature WGS reaction. A previous study showed that producing methanol from CO and water (through WGS) can be substantially more energy efficient than producing methanol from H<sub>2</sub> and CO<sub>2</sub>, through reverse water gas shift (RWGS); 62% compared to 49%. Given this downstream efficiency advantage, the baseline configuration considered here explores the WGS pathway to produce H<sub>2</sub> from CO to form synthesis gas for downstream conversion to methanol.<sup>15</sup>

The goal of the effort reported here is to analyze the baseline configuration beginning with sunlight, CO<sub>2</sub>, and water and ending with a liquid hydrocarbon fuel (methanol) with the intent of establishing a framework identifying major efficiency and cost drivers as well as environmental impacts and technology gaps. We intend to use this information to guide follow-on development and optimization efforts. As such, the effort here also establishes a baseline metric for product cost, lifecycle impacts, and process efficiency to which other routes and alternative unit operations can be compared. Additionally the work provides a system design tool for relating the performance of the solar thermochemical portion of the full process to the final output and therefore establishing performance guidelines and metrics. Future studies will exercise and expand upon this initial framework with a target of achieving double the baseline efficiency with commensurate cost reduction and lifecycle impact. Other than the Dish-CR5 components (solar concentrator/reactor subsystem), we base the full system here on well-established industrial processes and component designs to facilitate this baseline analysis and reduce uncertainties.

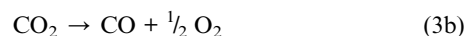
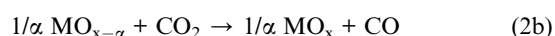
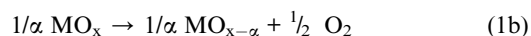
## 2. Process overview and subsystems

The general approach of the S2P project is the direct application of solar thermal energy to produce synthesis gas in a thermochemical metal oxide cycle as a pathway to liquid fuels. The particular process embodiment considered herein is based on the thermochemical splitting of CO<sub>2</sub> to produce CO and O<sub>2</sub>, the water gas shift reaction which allows the generation of H<sub>2</sub> from CO and H<sub>2</sub>O, and the methanol synthesis reaction which transforms H<sub>2</sub>, CO and CO<sub>2</sub> into methanol (MeOH).

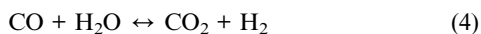
The thermochemical splitting of CO<sub>2</sub> considered in this analysis is based on an ultra-high temperature two-step iron oxide cycle that takes advantage of the concentrated solar flux. Iron oxide has been of interest since Nakamura described the FeO/Fe<sub>3</sub>O<sub>4</sub> cycle for water splitting.<sup>16</sup> The two steps in the archetype FeO/Fe<sub>3</sub>O<sub>4</sub> cycle are,



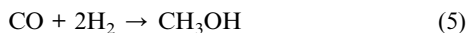
More generally the metal oxide redox cycle is:



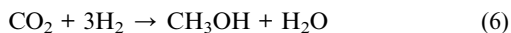
where M represents a reducible cation (*e.g.*, Ce or Fe). In either case, reaction 1 is the high temperature thermal reduction step, reaction 2 is the lower temperature re-oxidation step and reaction 3 represents the net carbon dioxide splitting reaction. Carbon monoxide produced in this way can then be used to produce hydrogen from water in the water gas shift (WGS) reaction (Reaction 4).



The resulting synthesis gas can be further converted to a liquid fuel in the methanol synthesis (MS) reactor.



Note that many kinetic models consider methanol synthesis (Reaction 5) to actually take place as a combination of the WGS reaction (Reaction 4) and  $\text{CO}_2$  hydrogenation (Reaction 6). That is, Reaction 4 occurs in the WGS reactor, but it also occurs in the MS reactor along with Reaction 6 wherein  $\text{CO}_2$  is the direct precursor to methanol.



This methanol producing process is used here in a baseline plant model that includes two separate facilities: the Dish-CR5 array, where  $\text{CO}_2$  is reenergized into CO using concentrated solar flux; and the main processing facility where the generated  $\text{CO}_2$ -CO mixture is transformed into methanol. Initial estimates indicate that the Dish-CR5 array will span approximately four square miles (about 10 km<sup>2</sup> or about 2,600 acres) to produce the desired flow rate of synthesis gas. The main processing facility is centered within the array and a suitable piping network interconnects the two. Fig. 1 shows a block flow diagram. The Dish-CR5 array is shown on the left. The main processing facility includes four subsystems: the water gas shift reaction loop, the amine-based  $\text{CO}_2$  absorption system, the methanol synthesis reaction loop, and the methanol purification system. For our baseline system, we chose a methanol production level equal to 82,700 Mg/year of 99% methanol product, which corresponds to an industrial-scale methanol plant and is equivalent to about 0.01% of US gasoline demand on an equivalent energy basis (378Mgal/day in 2009). Below we describe each of these subsystems in more detail.

## 2.1. Dish-CR5 array

The heart of this embodiment of the S2P process is the CR5. Shown in Fig. 2, the CR5 is a unique first generation solar chemical heat engine that allows for a continuous thermal reduction/oxidation cycle (reactions 1 and 2) with heat recuperation. Fins, consisting of the reactive material, such as YSZ-supported iron oxide<sup>8,10,11</sup> or ceria, are mounted on the counter-rotating rings at the outer radius. In the reduction zone of the reactor, concentrated solar flux from a parabolic dish provides both sensible heating of the fins and heat to drive the endothermic reduction reaction producing oxygen. As a ring rotates out of the reduction zone, it enters one of two heat

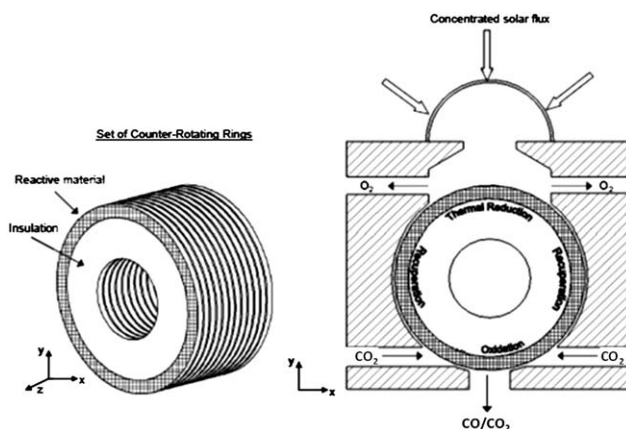


Fig. 2 CR5 schematic for  $\text{CO}_2$  splitting.

recuperation zones. In the recuperation region, the ring (hot) gives up heat to adjacent counter-rotating rings (cooler) through thermal radiation. At the end of the recuperation section, the ring enters the oxidation zone where the reactive material re-oxidizes and reduces gas phase  $\text{CO}_2$  to CO. The oxidized ring (now cool) then rotates into a second recuperator section where it now gains heat from the adjacent counter-rotating rings (hot) leaving the reduction zone. The pre-heated ring then enters the reduction zone and repeats the cycle.

This analysis considers CR5s containing 102 counter-rotating rings that are 36" in diameter. This geometry allows the rings to be counter-rotated at a rate between 0.5 and 1 rpm, depending on the reaction kinetics. Oxidation and reduction zone gases are kept separate by balancing pressure and flows. Carbon dioxide is introduced to the oxidation zone at multiple locations to maximize the oxidation extent of the reduced metal oxide. An excess amount of  $\text{CO}_2$  is delivered to the CR5 to also increase the reaction extent. This analysis assumes that approximately 25% of the  $\text{CO}_2$  is converted to CO. The resulting  $\text{CO}_2/\text{CO}$  stream is pumped away from the oxidation zone in the CR5 to the methanol production facility for  $\text{CO}_2$  separations and fuels synthesis.

Each CR5 is integrated with a single, 88 m<sup>2</sup> parabolic dish. The Dish-CR5 systems only operate 10 h per day when the required solar flux is available, but the methanol production facility operates continuously. An average solar insolation of 0.689 kW/m<sup>2</sup> (the average annual data in Daggett, California, US<sup>17</sup>) over the 10 h period was assumed for the analysis. This flux results in an average of 60.6 kW collected at each dish while on-sun. For the analysis that will be presented later, a solar to chemical (HHV  $\text{CO}/Q_{\text{solar}}$ ) energy conversion efficiency of 20% was assumed. With an assumed 50% solar collection efficiency (optical and thermal losses), 30.3 kW of usable thermal energy is available.

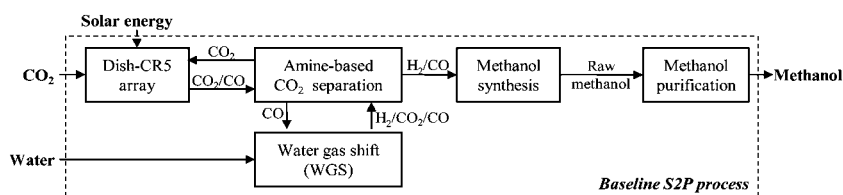


Fig. 1 Block flow diagram of the  $\text{CO}_2$ -to-methanol process.

12.1 kW is converted to CO chemical energy (20% of 60.6 kW) and the remainder accounts for incomplete heat recuperation and sensible heating of the product gas streams. To provide the gas flow rate required to produce 82,700 Mg/yr of 99% methanol, a large array of 17,622 Dish-CR5 systems is required, which collect 445 MW of solar flux per day. Conceptually, the array is laid out on a rectangular grid that is approximately 2 miles on a side with the methanol plant in the center. The precise size of an actual facility would of course scale with both the efficiency and the local solar resource. A piping network is used to move the CO<sub>2</sub>/CO streams from each dish to the central facility. Because the Dish-CR5 systems only operate 10 h per day, gas storage is required to feed the methanol production facility continuously.

An Aspen Plus model<sup>18</sup> has been assembled to represent the processes occurring within the CR5 as shown in Fig. 3. As described above, the CR5 contains three distinct processes; oxidation, reduction, and recuperation. In this model, the reactants are represented by a solid stream that passes through the oxidation and reduction reactors. The reduction product stream (hot) and the oxidation product stream (cool) are coupled by heat exchange to represent the recuperation regions of the CR5. The quantity of heat exchanged is defined by specifying a target temperature for the oxidation and reduction reactors and defining a recuperator efficiency. This assumes that the heat transfer coefficient is high enough and the heat capacity of the rings is low enough that we are able to attain adequate recuperation. In this current equilibrium model, kinetics are not explicitly included; the reaction is bounded by the available solar flux which determines the extent of the reduction reaction. The integration of this model with the plant model allows us to explore numerous sensitivities at the plant level, including CO production rate (dependent on the extent of reaction and material loading) as a function of solar insolation.

## 2.2. Water gas shift reaction system

The water gas shift reactor is used to convert steam and a portion of the CO produced by the CR5 into hydrogen based on the

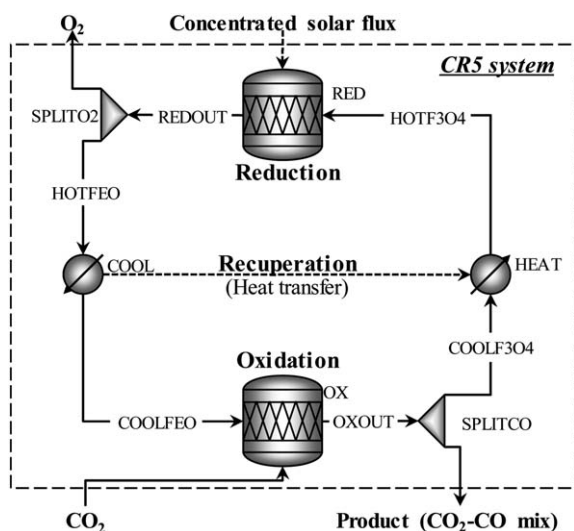


Fig. 3 Process flow diagram for representation of CR5.

reaction in eqn (4). We use an adiabatic fixed bed catalytic reactor, heaters and coolers to set proper reactor feed and effluent temperatures, and a simple flash vessel to separate the gas reaction products from excess water which is recycled back to the reactor. For the purposes of this study, a commercial Cu/ZnO/Al<sub>2</sub>O<sub>3</sub> catalyst is considered for the WGS reactor. This same catalyst is used in the methanol synthesis reactor described below. However, here the reaction conditions are selected to exclusively favor the WGS reaction. The gas phase reaction stoichiometry and kinetic expressions for this catalyst are presented in Table 1. The kinetic equation is a Langmuir-Hinshelwood type developed by Bussche and Froment.<sup>19</sup> The kinetics of the MS reaction reflects the fact that CO<sub>2</sub> is the immediate precursor to methanol and is a necessary component of the reaction mixture (reaction 6). The WGS system is designed to convert a fraction of CO to H<sub>2</sub> so that the production of methanol in the methanol reactor is maximized. In this study, this is achieved by a CO/CO<sub>2</sub>/H<sub>2</sub> molar ratio equal to 0.34/0.05/0.61.

## 2.3. Methanol synthesis reaction system

The methanol synthesis reactor is similar in concept to the WGS reactor and generates methanol from the synthesis gas mixture of CO, CO<sub>2</sub> and H<sub>2</sub> produced by the other plant subsystems. Like the WGS reactor, it is modeled as an adiabatic fixed bed catalytic reactor. The MS reactor system includes a simple flash vessel to separate and recycle unconverted gases increasing the carbon to methanol yield. In addition, operating conditions and feed composition were adjusted to maximize the carbon to methanol yield while maintaining a reasonable reactor size. Some studies indicate that water produced by MS remains attached to the active sites, poisoning the catalyst.<sup>20,21</sup> This problem is prevented through the use of the Cu/ZnO/Al<sub>2</sub>O<sub>3</sub> catalyst, which promotes WGS, and by having a large CO/CO<sub>2</sub> ratio in the reactor feed stream. Under proper conditions, this CO is consumed *via* WGS along with water, liberating active sites and producing more H<sub>2</sub> and CO<sub>2</sub> that later participate in the production of additional methanol.

## 2.4. Amine based CO<sub>2</sub> separation system

Both the MS and the WGS reactors achieve an optimum performance at specific CO<sub>2</sub>/CO molar ratios. To adjust these ratios, we employ an amine-based CO<sub>2</sub> separation system, which uses an aqueous solution of monoethanolamine (MEA) to absorb CO<sub>2</sub> in two different columns connected in series with a solvent regeneration column (a mature industrial process commonly used to remove CO<sub>2</sub> from coal fired power plants). Several important variables such as absorber temperature and pressure as well as the solvent CO<sub>2</sub> loading were optimized to lower the total capital and utility cost of the system.<sup>22</sup> The first column (see T-101 in Fig. 4) removes part of the CO<sub>2</sub> in the stream leaving the Dish-CR5 array, producing a rich CO mixture that is then fed to the WGS system. The objective here is to drive the WGS equilibrium to the production of H<sub>2</sub>. The second MEA column absorbs part of the CO<sub>2</sub> generated in the WGS system, producing a mixture with the required amount of CO<sub>2</sub> to optimally drive the MS reaction. The objective here is to drive the WGS equilibrium to counter the water poisoning while still



**Table 1** Kinetics expressions for Cu/ZnO/Al<sub>2</sub>O<sub>3</sub> catalyst: methanol synthesis (MS) reaction and reverse water gas shift (RWGS) reaction

$$\frac{\rho\omega^2 r_{av} d^2}{8\mu} r_{MS} = \frac{k_4 \cdot P_{CO_2} \cdot P_{H_2} \cdot \left(1 - \frac{1}{K_{MS}} \cdot \frac{P_{H_2O} \cdot P_{CH_3OH}}{P_{H_2}^3 \cdot P_{CO_2}}\right)}{\left(1 + k_3 \cdot \frac{P_{H_2O}}{P_{H_2}} + k_1 \cdot \sqrt{P_{H_2}} + k_2 \cdot P_{H_2O}\right)^3}, \quad r_{RWGS} = \frac{k_5 \cdot P_{CO_2} \cdot \left(1 - \frac{1}{K_{RWGS}} \cdot \frac{P_{H_2O} \cdot P_{CO}}{P_{H_2}^3 \cdot P_{CO_2}}\right)}{\left(1 + k_3 \cdot \frac{P_{H_2O}}{P_{H_2}} + k_1 \cdot \sqrt{P_{H_2}} + k_2 \cdot P_{H_2O}\right)}$$

$$K_{MS} = 10^{\left[\frac{3066}{T} - 10.592\right]} \quad k_1 = 0.499 \cdot e^{\frac{17197}{R \cdot T}} \quad k_4 = 1.07 \cdot e^{\frac{36696}{R \cdot T}}$$

$$K_{RWGS} = 10^{\left[\frac{-2073}{T} + 2.029\right]} \quad k_2 = 6.62E - 11 \cdot e^{\frac{124119}{R \cdot T}} \quad k_5 = 1.22E10 \cdot e^{\frac{-94765}{R \cdot T}}$$

$$k_3 = 3453.38 \quad r_{MS}, r_{RWGS} [=] \text{mol}/(\text{kg}_{cat} \cdot \text{s}) \quad T [=] \text{K}, \quad P [=] \text{bar}$$

favoring the MS equilibrium as to obtain an optimum carbon to methanol yield. The regeneration column strips the absorbed CO<sub>2</sub> from the MEA allowing solvent reuse and CO<sub>2</sub> recycling to the Dish-CR5 array. In addition to removing CO<sub>2</sub> to optimize reaction yields, the MEA system reduces the total flow going through the reaction loops, which means lower capital and operational costs (smaller pieces of equipment and lower cooling/heating utility consumption). Finally, we performed heat integration to reduce the heating duty of the regenerating column.

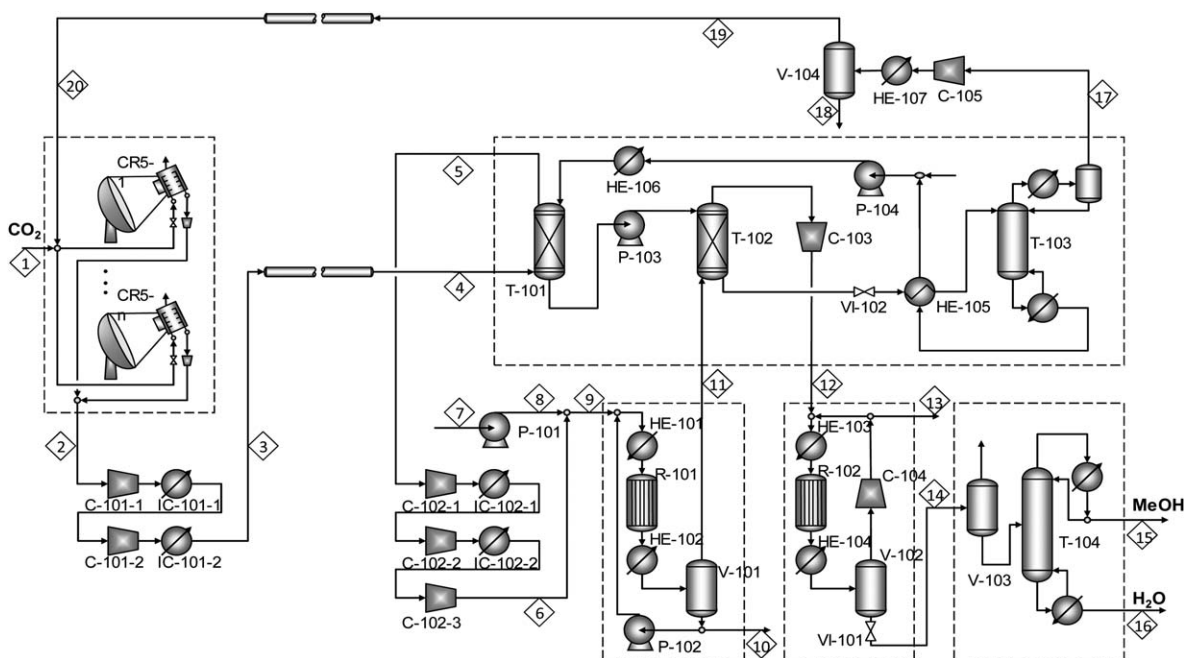
### 2.5. Methanol purification system

The final subsystem in our process is the methanol purification system. This system separates incondensable materials (*i.e.* CO<sub>2</sub>, CO, H<sub>2</sub>) and water from the methanol. The system includes a simple flash vessel to separate light materials and a standard distillation column to perform the methanol-water separation.

### 3. Process development

Fig. 4 shows the plant layout with numbered process streams and components to facilitate the process flow description. This process represents an improvement over the traditional “Carbon dioxide hydrogenation to form Methanol *via* REverse water-gas shift reaction” (CAMERE) process,<sup>20</sup> since it shares the same production and environmental benefits (*e.g.* MeOH production and CO<sub>2</sub> recycling) while using solar power, instead of very costly H<sub>2</sub>. For the synthesis and analysis of the integrated process we developed a process simulation model in Aspen Plus.<sup>18</sup>

The capacity of the process is approximately 82,700 Mg/yr of 99% mole methanol product (*i.e.*, 81,925 Mg/yr of pure CH<sub>3</sub>OH). Assuming that the facility operates 333 days per year, this leads to 7,742 kmol/day of methanol product or 7,670 kmol/day of pure CH<sub>3</sub>OH. To satisfy this production rate, an array of 17,622 Dish-CR5 units is fed with a CO<sub>2</sub> stream (1) carrying 10,344

**Fig. 4** Simplified process flow diagram.

kmol/day of CO<sub>2</sub> at 25 °C and 1 bar. This feed stream is combined with a CO<sub>2</sub> recycle stream (20) carrying 92,880 kmol/day of CO<sub>2</sub> from the amine separation system. Each CR5 unit converts 24.5% of the CO<sub>2</sub> to CO for a total CO flow rate of 25,320 kmol/day (1.437 kmol CO/day/CR5). The resulting CO–CO<sub>2</sub> product streams are combined into a single process stream (2) that is brought to 7 bar using compression train C-101, and sent to the main processing facility through the piping network. At the processing facility, the CO–CO<sub>2</sub> stream (4) enters absorber T-101 where part of the CO<sub>2</sub> is removed, adjusting the CO/CO<sub>2</sub> molar ratio to 0.9/0.1. The resulting CO rich mixture (5) is brought to 50 °C and 22 bar by the compressor train C-102 and mixed with a H<sub>2</sub>O stream (7) (16,176 kmol/day) to produce the feed (9) to the WGS system. This feed temperature is set to 280 °C by HE-101 before it enters the WGS reactor R-101. In this reactor, a fraction of the original CO reacts with H<sub>2</sub>O to produce CO<sub>2</sub> and H<sub>2</sub> required for methanol synthesis. The reaction product stream is now cooled to 35 °C by HE-102 and the unreacted water is separated at V-101 from the remaining light components CO, CO<sub>2</sub>, and H<sub>2</sub>. This gas stream (11) is now passed through the absorber T-102 to strip a fraction of the CO<sub>2</sub> content, adjusting the CO/CO<sub>2</sub>/H<sub>2</sub> molar ratio to 0.34/0.05/0.61. The stream is then further compressed to 47 bar by the single-stage compressor C-103 and fed to the MS system. In this system, the mixture (12) is brought to 210 °C by HE-103 before entering the methanol synthesis reactor R-102, where CO<sub>2</sub> reacts with H<sub>2</sub> to produce methanol and H<sub>2</sub>O. The H<sub>2</sub>O reacts with CO *via* WGS to produce additional CO<sub>2</sub> and H<sub>2</sub> which in turn produce more methanol. The MS reactor product is then cooled to 35 °C in HE-104 and the resulting methanol-water mixture (14) is separated at V-102 from the remaining light components CO, CO<sub>2</sub>, and H<sub>2</sub>. Most of this vapor product is recycled to R-102 in order to increase the carbon to methanol yield, while the rest (13)

is discarded. The methanol-water mixture (14) is first expanded to 3 bar at V-103 in order to separate traces of incondensable materials. The liquid mixture is finally separated at distillation column T-104 with a partial condenser, generating the methanol product stream (15) (7,742 kmol/day) and some waste water (16). The CO<sub>2</sub>-rich solvent stream generated in absorption towers T-101 and T-102 is sent to T-103 for regeneration. First, however, the stream is expanded through VI-102 and heated in HE-105. The outputs of T-103 are a CO<sub>2</sub>-lean solvent stream that is circulated back to T-101, and a CO<sub>2</sub>-rich vapor stream (17) carrying the 92,880 kmol/day of CO<sub>2</sub> which is recycled back (19–20) to the Dish-CR5 array after compression to 7 bar in C-105, cooling to 97 °C in HE-107 and H<sub>2</sub>O separation in vessel V-104.

#### 4. Energy efficiency analysis

In this study, we calculate four types of energy efficiencies, as shown in Table 2. The net energy efficiency is calculated as the ratio of the chemical energy of the product (MeOH) to the chemical energy of energized CO plus the energy provided by utilities, where we assumed that the high heating value (HHV) of MeOH is 726MJ/Kmol. The net energy efficiency is equal to 24.3%. The gross energy efficiency is calculated as the ratio of the chemical energy of the product to the total energy entering the system assuming that process heat and electricity are supplied externally from a utility plant. Gross energy efficiency is equal to 10.4%. We then calculate two primary energy efficiencies assuming that process heat and electricity are generated on-site. We examine two scenarios:

(1) Process heat is generated from natural gas and electricity is generated according to the 2009 US electricity mix (see Table 2). This is the conventional process, henceforth referred to as S2P-C process.

**Table 2** Energy efficiency of the MeOH production plant (capacity = 82,700 Mg/yr); energy consumption expressed in kW

Energy consumption	
A. Solar energy collected ( $Q_{solar}$ )	439,584
B. Energy incorporated into CO <i>via</i> CO <sub>2</sub> splitting <sup>a</sup> ( $Q_{CO}$ )	87,917
C. Process heat and electricity ( $E_{sys}$ )	176,816
Electricity	28,294
Heat	148,521
D. Heat of reaction of the produced MeOH ( $Q_{MeOH}$ )	64,310
E. Net energy efficiency [=D/(B + C)] (%)	24.3
F. Gross energy efficiency [=D/(A + C)] (%)	10.4
Primary energy consumption – conventional generation (S2P-C)	
Conventional resources to electricity <sup>b</sup>	76,471
Natural gas to heat <sup>c</sup>	172,699
G. Primary energy for process heat and electricity	249,170
H. Primary energy efficiency [=D/(A + G)] (%)	9.3
Primary energy consumption – generation from solar (S2P-S)	
Solar to electricity <sup>d</sup>	141,472
Solar to heat <sup>e</sup>	330,048
I. Solar equivalent energy for process heat and electricity	471,519
J. Primary solar-equivalent energy efficiency [=D/(A + I)] (%)	7.1

<sup>a</sup> Solar-to-chemicals efficiency: 20%. <sup>b</sup> Conventional resources to electricity efficiency: 32–38% depending on the energy mix; 37% is used. In this study we assumed the following energy mix (US 2009 mix): coal (45%), natural gas (23%), nuclear (20%), hydro (7%), renewable and others (4%), and oil (1%).<sup>1</sup>  
<sup>c</sup> Natural-gas-to-heat efficiency: 85–90% depending on feedstock composition and capacity; 86% is assumed. <sup>d</sup> Solar-thermal-to-electricity efficiency: 18–23%; 20% is assumed. <sup>e</sup> Solar-thermal-to-heat efficiency: 47–55%; 50% is assumed.

(2) Process heat and electricity are generated from solar energy. This *solar-only* process will be referred to as S2P-S process.

In the conventional scenario, the primary energy efficiency is equal to 9.3%, while in the solar only scenario, it is equal to 7.1%.

If we compare this 7.1% primary energy efficiency to other alternative energy approaches, we find that it is competitive. Until now, most chemical schemes (*i.e.* excluding those best categorized as “artificial photosynthesis”) envision water electrolysis serving as the primary process for converting renewable energy to chemical energy.<sup>23–26</sup> That is, water is split by electrical energy and H<sub>2</sub> is the key energetic chemical intermediate. A number of analyses of this H<sub>2</sub>-based approach have been carried out with varying levels of detail. A high-level analysis suggested that methanol could be produced from sunlight at an overall efficiency of greater than 13%.<sup>23</sup> More detailed process work indicated that an overall electric to hydrocarbon fuel efficiency in the range of 42–51% could be achieved with current technology, accounting for the fraction of process heat allotted for CO<sub>2</sub> recovery as an equivalent loss of electrical power generation at the fossil-fueled power plant generating the recovered CO<sub>2</sub>.<sup>26</sup> With a time-averaged solar to electrical efficiency of 10% (a reasonable assumption for photovoltaics) or 20% (for solar thermal electric), these results suggest a range of 4–10% solar to fuel efficiency is currently achievable. Note that even the lower end of this range, while small, is still significantly higher than that achieved by biomass approaches, which are limited by the inefficiency of photosynthesis.

At 7.1% solar to fuel efficiency, our baseline plant utilizing no primary energy source other than solar already falls within the efficiency range of the electrolytic pathways. However, our analysis has identified several high leverage opportunities to achieve substantially better system or primary efficiencies. With the assumption of 20% solar to chemical efficiency, the Dish-CR5 subsystems limit the upper end. However, the current efficiency can be increased substantially with process improvements that reduce heat requirements. Examples of such improvements include more efficient gas separations, better heat integration between plant process units, and alternative syngas pathways such as water splitting or combined CO<sub>2</sub> and water splitting.

## 5. Environmental impact analysis

To assess the environmental impact of this baseline system we performed a “cradle-to-gate” life cycle assessment (LCA) from resource extraction (cradle) to the plant gate (*i.e.*, before MeOH is transported to the pump). Accordingly, the system boundary includes construction, fuel production, and disassembly phases of the MeOH production plant as shown in Fig. S1, in supplementary information.† The LCA inventory is calculated for three processes (component inventory data are provided in Tables S1 and S2 in supplementary information†):

- *Classical-NG process*: Conventional MeOH production from natural gas (NG), which consists of four sub-processes: steam reforming of natural gas, syngas purification, MeOH synthesis, and MeOH separation.

- *S2P-C process*: The baseline configuration process in this study with utilities (heat and electricity) generated from conventional fuels.

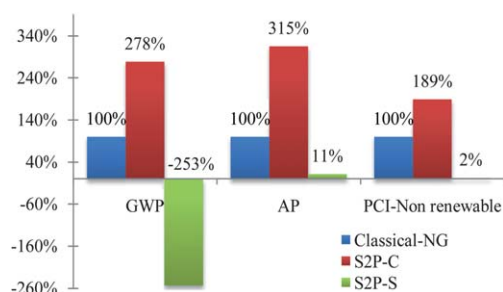


Fig. 5 Environmental impact and non-renewable energy consumption of the S2P processes compared to the classical-NG process.

- *S2P-S process*: The S2P process with utilities generated from solar energy.

In a life cycle impact assessment (LCIA), various environmental impact categories may be considered (*e.g.*, global warming, acidification, ozone depletion, eutrophication and human/ecological toxicity). Here we focus only on the anticipated largest impacts, global warming potential (GWP) and acidification potential (AP). In addition, primary energy consumption is assessed using the primary comparative indicator (PCI). These three terms, GWP, AP, and PCI are defined as:

- *Global warming potential (GWP)*: The impact of greenhouse gases (GHGs). For simplicity, only the three most relevant GHGs are considered, namely: CO<sub>2</sub>, CH<sub>4</sub> and N<sub>2</sub>O. The amount of CH<sub>4</sub> and N<sub>2</sub>O emitted is converted into CO<sub>2</sub> equivalent (kg CO<sub>2</sub>-eq.).

- *Acidification potential (AP)*: The impact from emissions of acidifying pollutants, mainly SO<sub>2</sub>, NO<sub>x</sub> and NH<sub>4</sub>. The acidification potential for every acidifying emission to the air is converted into SO<sub>2</sub> equivalent (kg SO<sub>2</sub>-eq.).

- *Primary comparative indicator (PCI)*: The total primary energy requirement (kWh/kg MeOH) which is used to indicate primary energy consumption.<sup>27</sup> Here we study non-renewable primary energy requirements.

Fig. 5 shows a comparison of environmental impact and energy consumption of the two S2P processes, normalized with respect to the classical-NG process. Despite the advantage of directly using CO<sub>2</sub> as a raw material, the GWP and AP of the S2P-C process are higher than those of the classical-NG process due to the high heat requirement of the conventional CO<sub>2</sub> separation system. However, if heat and electricity are generated using solar energy, like in the S2P-S process, the GWP and AP are dramatically reduced. Since the consumption of solar energy has minimal GWP, the consumption of CO<sub>2</sub> as a raw material leads to a negative GWP and small AP impacts for the S2P-S process. The S2P-C process has a large PCI of non-renewable energy compared to the classical-NG process because a significant amount of non-renewable energy is used for CO<sub>2</sub> separation. However, the PCI for non-renewable energy of the S2P-S process is almost zero because there is no non-renewable energy consumption in the fuel production phase. The total PCI, which includes non-renewable and renewable energy, of the two S2P processes is higher than the classical-NG process due to the low solar-to-chemicals efficiency (see Table S3 in supplementary information†). As expected a chemical to chemical conversion is more efficient than a solar to chemical conversion.

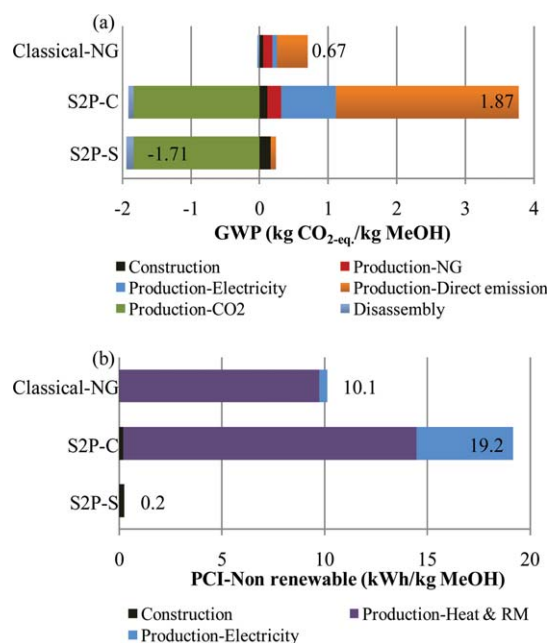


**Fig. 6** Contributions of construction, manufacturing and disassembly phase. (a) Global warming potential. (b) Primary comparative indicator for non-renewable resources (RM: raw material; NG: natural gas).

The contributions of the three major phases in the life cycle of the plants (construction, fuel production, and disassembly) to the GWP and PCI for non-renewable energy are shown in Fig. 6. First, we note that in the Classical-NG and S2P-C processes, the fuel production phase accounts for more than 97% of GWP and 98% of PCI. In the S2P-S process, the construction phase is dominant because direct emissions are negligible and there is no non-renewable energy consumption. In terms of GWP, direct emissions (*e.g.*, flue gases) are the major contributors in both the NG-Classical and S2P-C processes. The second contributor in the conventional process is natural gas supply, including extraction and transport, while in the S2P-C process it is electricity generation. The GWP of the S2P-S process is negative. In terms of primary non-renewable energy consumption, the use of natural gas as a raw material and heating source (9.7 kWh/kg MeOH) is the major contributor in the classical-NG process as shown in Fig. 6(b). In the S2P-C process, the use of natural gas to generate process heat is the highest contributor followed by electricity consumption; these utilities account for 98.9% of the total non-renewable energy requirement. Changing to utilities from solar energy leads to a large reduction; only 0.2 kWh/kg MeOH is used during the construction phase of the S2P-S process. Similarly, substantially reducing the utility load with different separations, combined CO<sub>2</sub> and water splitting, and heat integration would significantly reduce the GWP and PCI of an S2P-C configuration.

This preliminary LCA, while limited due to the early stage of development of the S2P concept, indicates that our baseline process with solar-based utilities is a significant improvement over conventional MeOH production from natural gas. The net GWP is negative and the use of non-renewable energy resources is negligible.

**Table 3** Economic evaluation parameters

Project's economic life [yr]	30
Working capital [% of capital expense]	5%
Operating charges [% of operating labor cost <sup>a</sup> ]	15%
Plant overhead [% of labor and maintenance costs]	25%
Desired rate of return [%/yr]	8%
Tax rate [%/yr]	35%
Salvage value [% of capital cost]	20%
Depreciation	Straight line
Capital escalation [%/yr]	5%
Raw material escalation [%/yr]	2%
Product escalation [%/yr]	5%
Utility escalation [%/yr]	2%

<sup>a</sup> Labor cost includes operator (20 USD/person/h) and supervisory (35 USD/person/h) costs. Calculation based on number of operators per shift, wage rate, and operating hours per year.

## 6. Economic evaluation

An economic feasibility study was performed for the baseline system described above. The capital and operational costs of the various process subsystems are identified and the break-even price of methanol is determined. To this end, nominal prices of CO<sub>2</sub>, H<sub>2</sub>O and MeOH were used according to recent technology analysis and market trends. Detailed Net Present Value (NPV) sensitivity analysis studies were also performed using Aspen Process Economic Analyzer.<sup>18</sup> We assumed the plant to be new (grass roots) and constructed in North America. The most important evaluation parameters are given in Table 3.

The raw material and product prices as well as the utility costs we considered are as follows:

- *CO<sub>2</sub> price*: Several studies identify amine absorption as one of the most economic systems for CO<sub>2</sub> capture. Using this technology the price of CO<sub>2</sub> coming from a capture unit in a power station is around 35 USD/Mg CO<sub>2</sub>.<sup>22</sup>
- *H<sub>2</sub>O price*: The price considered here was the standard value of de-ionized water; that is, 1 USD/Mg.
- *MeOH price*: Methanol price has a highly fluctuating behavior. For this particular study 449 USD/Mg was considered; the value is the MNDRP (methanex non-discounted reference price) in January, 2011 from www.methanex.com.
- The process consumes four types of utilities, the prices of which are given in Table 4. We assume here that the broader goal of renewable utilities reaching parity with conventional utilities will be achieved.

A summary of the economic evaluation based on the parameters and prices listed above is given in Table 5. The capital expenditure for the project is around 614.5 million USD resulting in an annualized capital cost of 54.6 million USD/year. The total operating cost including raw materials and utilities is 45.7 million USD/year. Both of these values exceed the methanol sales of 37.1 million USD/year resulting in a negative NPV.

**Table 4** Utility prices for MeOH production plant

Electricity [USD/kWh]	0.06
Low pressure steam [USD/Mg]	10.50
High pressure steam [USD/Mg]	14.50
Cooling water [USD/m <sup>3</sup> ]	0.03



**Table 5** Economic evaluation summary

Project time horizon [yr]	30
Total project capital cost [USD]	614,501,000
Annualized capital cost [USD/yr] <sup>a</sup>	54,567,770
Total operating cost [USD/yr] <sup>b</sup>	45,717,000
Total products sales [USD/yr] <sup>b</sup>	37,134,064
Project net present value (NPV) [USD]	-640,251,516

<sup>a</sup> Annualized capital cost (ACC) = CRF (capital recovery factor) × TPCC (total project capital cost). CRF is calculated by the following equation:  $CRF = i \times (i + 1)^N / [(i + 1)^N - 1]$ . Where  $i$  is annual discount rate on loans and  $N$  is operation time of the system in consideration. In this study, we assumed  $i = 8\%$  and  $N = 30$  years; thus,  $CRF = 0.0888$ . <sup>b</sup> Average value over the life of the project; expressed at present time.

### 6.1. Capital and operating costs

Excluding the Dish-CR5 units, standard sizing and costing algorithms within Aspen Process Economic Analyzer were used to determine capital costs from material and energy balances.<sup>18</sup> The Dish-CR5 array was sized and its cost calculated as presented in Tables S4 and S5 in supplementary information.† The capital cost breakdown in Fig. 7 (a) shows that the Dish-CR5 array direct cost is the dominant capital cost component. This is due to the significant cost of the parabolic dishes (which accounts for more than 80% of the direct cost of every Dish-CR5 unit), and the high number of units required to supply the main processing facility with the CO needed to maintain the MeOH production capacity. Thus, the total capital cost can be reduced if the Dish-CR5 unit cost is lowered or if the required number of units is reduced, which would require an improvement in the solar to chemical conversion efficiency currently assumed to be 20%. While this is theoretically possible, it may be difficult to achieve in practice, especially considering the 20% is already an

aggressive practical target, although well below what is theoretically possible. Alternatively, decreasing the cost of a parabolic concentrator *via* design and materials improvements is the subject of current development efforts, *e.g.* for Stirling cycle electric power generation. Finally, the unit capital cost can be reduced if the CO<sub>2</sub>-to-methanol conversion (currently at 75%) is improved.

In the case of operating costs, the amine CO<sub>2</sub> separation system is the highest contributor followed by the CR5 system. This is due to the high energy consumption required to regenerate the amine solvent, and the electricity consumed by the small vacuum pump/compressors in each CR5 unit. Table 6 presents a breakdown of utility consumption in terms of utility type and the contribution of each type to the cost of methanol. Table 7 presents the contribution of the different processing subsystems to the total utility costs. As the single highest contributor to operating costs, higher efficiency separations would have a large impact. To this end, improved separation technologies are being pursued as part of the S2P project. In addition, better heat integration between plant processes is being investigated. In order to reduce the utility costs associated with the CR5 compressors the total gas load would need to be reduced or a more efficient compression scheme developed. Both options are currently being studied.

### 6.2. Sensitivity analysis

To study the impact of raw material and product prices on the economic performance of the project, NPV calculations were conducted for different scenarios. The results indicate that the NPV sensitivity with respect to the CO<sub>2</sub> price is much lower than its sensitivity with respect to the price of MeOH. We also determined that a change in the CO<sub>2</sub> price alone cannot lead to profitable operation. However, it is important to remember that if emission regulations or emission trading schemes are introduced, CO<sub>2</sub> consumers will get credits, which would improve the economics of the proposed technology.

Fig. 8 presents the sensitivity of the project NPV with respect to the price of methanol. If nominal values are used for all evaluation parameters (including the price of CO<sub>2</sub>), a methanol price of 1.22 USD/kg would be required to reach the break-even point, which is higher than the current methanol price (produced primarily from natural gas). As previously discussed, reductions in the cost of parabolic dishes and improved gas separations are the biggest levers to improve the plant economics. Note that a large percentage of our costs are derived from capital expenditures and that this should provide some measure of stability and relative gains as the price of fossil feedstocks increase.

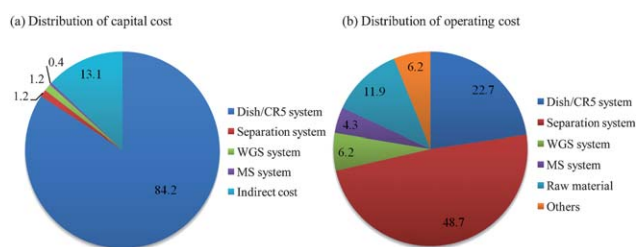


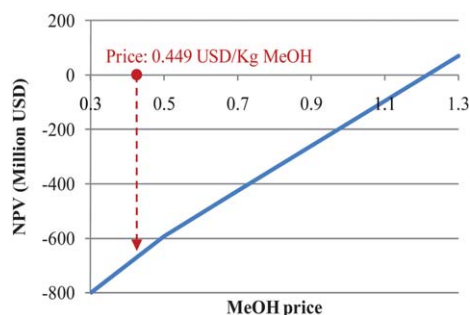
**Fig. 7** Distribution of capital cost and operating cost for the methanol production process. Indirect costs include engineering and supervision costs, construction expenses, other expenses, and contingency.

**Table 6** Total utility consumption and costs

	Consumption/Year		Value/Year	
	Quantity	Units	Total cost (USD)	USD/kgMeOH
Electricity	236,146,400	kWh	14,168,784	0.17
Low pressure steam	1,859,906	Mg	19,529,017	0.24
High pressure steam	32,824	Mg	475,942	0.01
Cooling water	103,269,680	m <sup>3</sup>	3,273,649	0.04
Total			37,447,392	0.45

**Table 7** Utility cost distribution

Part	Total utility cost (USD)	Percent (%)
Dish/CR5 system	10,368,530	27.7
Integrated separation system	22,274,456	59.5
WGS reaction system	2,843,921	7.6
MS reaction system	1,960,486	5.2

**Fig. 8** Project NPV sensitivity to MeOH price.

## 7. Conclusions

Chemical schemes for converting CO<sub>2</sub> and H<sub>2</sub>O to liquid hydrocarbons are a necessary component of a future energy mix if we are to find scalable alternatives to petroleum for transportation. Potential advantages for the solar chemical schemes include a more direct pathway to the desired end-product accompanied by higher overall efficiency thereby side-stepping resource limitations, especially land and water. A key challenge will be driving down the cost of producing the end product, most specifically the cost of collecting the solar flux.

We have examined a baseline configuration of a solar thermochemical scheme for converting CO<sub>2</sub> and H<sub>2</sub>O to a liquid hydrocarbon fuel. In contrast to the electrochemical approach, the fundamental chemistry behind the process considered here includes the solar thermochemical splitting of CO<sub>2</sub> into CO, the production of H<sub>2</sub> from CO using the water gas shift reaction, and finally the synthesis of methanol from syngas, namely a mix of H<sub>2</sub>, CO, and CO<sub>2</sub>. A techno-economic evaluation of this baseline process suggests that a solar-to-methanol energy efficiency of 7.1% is feasible *via* this baseline approach, assuming the dish-CR5 units can achieve a 20% sunlight to CO energy conversion efficiency. Our analysis further indicates that for profitability, the selling price of methanol produced *via* this not yet optimized baseline approach would need to be no less than 1.22 USD/kg, pricing solar utilities at grid parity. “Cradle-to-gate” LCA indicates that the solar-driven process offers significant advantages in terms of GWP, AP, and non-renewable PCI.

The baseline, non-optimized efficiency compares favorably with the electrochemical approach, but the cost is higher than the current market price (0.45 USD/kg) as is true for electrochemical-based approaches. However, this work has highlighted the cost-drivers and technology gaps and shows that there are many opportunities to optimize the system design. These will be addressed in future work to improve over the baseline efficiency, LCA, and economics.

For example, reducing the cost of solar collection, in this case parabolic dish systems, has high leverage impact on the economics. Because of the diffuse nature of sunlight, this is likely to be true for any solar-driven fuel-producing scheme. In this regard, the solar thermochemical approach is poised to benefit from commercialization and advances in adjacent solar electric technologies such as dish-Stirling electric generation. Additionally, increasing the energy efficiency of the CR5, thereby lowering the total number of Dish-CR5 units required, would have significant impact. Beyond capital costs, the analysis indicated that operating costs for the current configuration are dominated by the heat burden for the MEA-based CO<sub>2</sub> separations. The heat burden also looms large in the S2P-C LCA case wherein conventional utilities are applied to plant operations. The utilities negate the gains of the solar splitting process in terms of GWP and AP; in the absence of significant improvements, utilities would be required to be renewable as in the solar-only option, S2P-S. To some extent, this burden can be mitigated by better heat integration from the system into the MEA process. However, alternative separations, and the combination of solar thermochemical CO<sub>2</sub> and water splitting (avoiding water-gas-shift and the associated recycle), provide significant and likely larger opportunities to increase the system efficiency. Increasing the per-pass CO<sub>2</sub> to CO yield, *i.e.* increasing the concentration of CO (decreasing the total flow rate) in the dish effluent for a given efficiency, would also influence the size and cost of operating the separation units.

In summary, this study provides a baseline system and suite of tools for assessing system energy efficiency, environmental impact, and economics for the S2P process and points towards cost and environmental drivers and technology gaps. Although the baseline system is already reasonably promising, further improvements beyond these baseline values are critical to avoid resource limitations (*e.g.* minimize land requirements) and to minimize the capital investment associated with capturing the solar resource, and minimize utilities consumption. Future studies will build upon this framework to determine the system efficiency, lifecycle assessment, and cost impact of different process configurations, alternate unit operations, different end products, and additional process integration and distribution. Follow on work will consider a number of advanced system configurations, with the goal of demonstrating at least a doubling of the energy efficiency over the baseline.

## Acknowledgements

This work was supported by the Laboratory Directed Research and Development program at Sandia National Laboratories, in the form of a Grand Challenge project entitled Reimagining Liquid Transportation Fuels: Sunshine to Petrol. Sandia is a multiprogram laboratory operated by Sandia Corporation, a Lockheed Martin Company, for the United States Department of Energy’s National Nuclear Security Administration under Contract DE-AC04-94AL85000.

## Reference

- 1 U.S. Energy Information Administration, *Annual Energy Review-2009*, 2009.
- 2 X. Xiaoding and J. A. Moulijn, *Energy Fuels*, 1996, **10**, 305–311.

- 3 H. Arakawa, M. Aresta, J. N. Armor, M. A. Barteau, E. J. Beckman, A. T. Bell, J. E. Bercaw, C. Creutz, E. Dinjus, D. A. Dixon, K. Domen, D. L. DuBois, J. Eckert, E. Fujita, D. H. Gibson, W. A. Goddard, D. W. Goodman, J. Keller, G. J. Kubas, H. H. Kung, J. E. Lyons, L. E. Manzer, T. J. Marks, K. Morokuma, K. M. Nicholas, R. Periana, L. Que, J. Rostrup-Nielson, W. M. H. Sachtler, L. D. Schmidt, A. Sen, G. A. Somorjai, P. C. Stair, B. R. Stults and W. Tumas, *Chem. Rev.*, 2001, **101**, 953–996.
- 4 National research council, *Carbon management: implications for R&D in the chemical sciences and technology*. National Academies Press, Washington, D.C, 2nd edn, 2001.
- 5 M. Aresta and E. Kluwer, *Carbon dioxide recovery and utilization*, Academic Publishers, Dordrecht, Netherlands, 2003.
- 6 C. Song, *Catal. Today*, 2006, **115**, 2–32.
- 7 M. Aresta and A. Dibenedetto, *Dalton Trans.*, 2007, 2975–2992.
- 8 J. E. Miller, R. B. Diver, N. P. Siegel, E. N. Coker, A. Ambrosini, D. E. Dedrick, M. D. Allendorf, A. H. McDaniel, G. L. Kellogg, R. E. Hogan, K. S. Chen and E. B. Stechel, Sunshine to Petrol: A Metal Oxide Based Thermochemical Route to Solar Fuels, *The Minerals, Metals & Materials Society (TMS) annual meeting & Exhibition: Session I*, 2010.
- 9 R. B. Diver, J. E. Miller, M. D. Allendorf, N. P. Siegel and R. E. Hogan, *J. Sol. Energy Eng.*, 2008, **130**, 041001–1.
- 10 R. B. Diver, N. P. Siegel, T. A. Moss, J. E. Miller, L. Evans, R. E. Hogan, M. D. Allendorf, J. N. Stuecker and D. L. James, SAND2008–0878, 2008.
- 11 J. E. Miller, SAND2007–8012, 2007.
- 12 J. E. Miller, M. D. Allendorf, R. B. Diver, L. R. Evans, N. P. Siegel and J. N. Stuecker, *J. Mater. Sci.*, 2008, **43**, 4714–4728.
- 13 E. N. Coker, M. A. Rodriguez, A. Ambrosini, R. R. Stumpf, E. B. Stechel, C. Wolverton and B. Meredig, SAND2008–7655, 2008.
- 14 J. E. Miller, L. R. Evans, N. P. Siegel, R. B. Diver, F. Gelbard, A. Ambrosini and M. D. Allendorf, SAND2009–0399, 2009.
- 15 C. A. Henao, C. T. Maravelias, J. E. Miller and R. A. Kemp, *Design for Energy and the Environment: Proceedings of the 7th International Conference on the Foundations of Computer-Aided Process Design*, CRC Press, Boca Raton, Fla, 2010, 795–803.
- 16 T. Nakamura, *Sol. Energy*, 1977, **19**, 467–475.
- 17 G. Simons and J. McCabe, CEC-500-2005-072-D, 2005.
- 18 *Aspen Plus, Version 7.0*, Aspen Technology Inc., Cambridge, MA, 2008; *Aspen Process Economic Analyzer, Version 7.0*, Aspen Technology Inc., Cambridge, MA, 2008, <http://www.aspentech.com>.
- 19 K. M. Vanden Bussche and G. F. Froment, *J. Catal.*, 1996, **161**, 1–10.
- 20 O. Joo, K. Jung, I. Moon, A. Y. Rozovskii, G. I. Lin, S. Han and S. Uhm, *Ind. Eng. Chem. Res.*, 1999, **38**, 1808–1812.
- 21 O. Joo, K. Jung, Y. S. Jung, *Carbon Dioxide Utilization for Global Sustainability*, 2004, 153, 67–72.
- 22 C. Alie, L. Backham, E. Croiset and L. Douglas, *Energy Convers. Manage.*, 2005, **46**, 475–487.
- 23 T. Weimer, K. Schaber, M. Specht and A. Bandi, *Energy Convers. Manage.*, 1996, **37**, 1351–1356.
- 24 G. A. Olah, A. Goeppert and G. K. S. Prakash, *J. Org. Chem.*, 2009, **74**, 487–498.
- 25 D. Mignard, M. Sahibzada, J. M. Duthie and H. W. Whittington, *Int. J. Hydrogen Energy*, 2003, **28**, 455–464.
- 26 D. Mignard and C. Pritchard, *Trans. IChemE A.*, 2006, **84**, 828–836.
- 27 H. Baumann and A. M. Tillman. *The Hich Hiker's Guide to LCA – An orientation in life cycle assessment methodology and application*, Studentlitteratur, Lund, 1st edn, 2004.